Supporting Information Available in Web Edition

Two types of quasi-liquid layers on ice crystals are formed kinetically

Harutoshi Asakawa[†], *Gen Sazaki*[*], *Ken Nagashima, Shunichi Nakatsubo, Yoshinori Furukawa*

Institute of Low Temperature Science, Hokkaido University, N19-W8, Kita-ku, Sapporo 060-0819, Japan

Contents

References

Other Supporting Online Material for this manuscript includes Videos S1, S2 and S3.

† Present address: Department of Creative Technology Engineering, National Institute of Technology, Anan College, 265 Aoki Minobayashi, Anan, Tokushima 774-0017, Japan

* To whom correspondence should be addressed. E-mail: sazaki@lowtem.hokudai.ac.jp

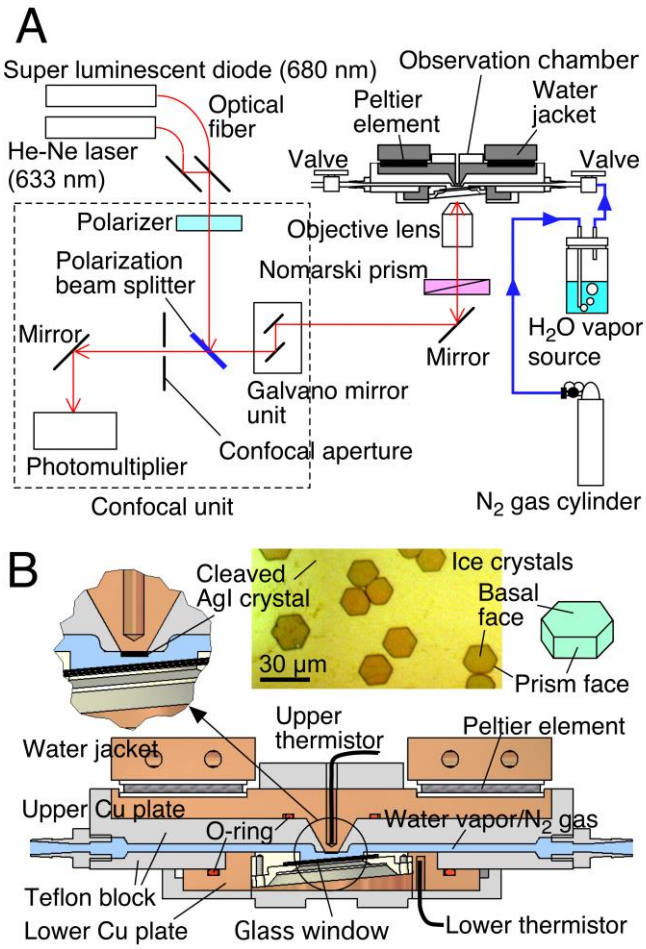

Fig. S1. Schematic drawings of the experimental setups (this Figure was reprinted from Fig. S2 of ref. (12)). (A) The LCM−DIM system, the observation chamber and the water−vapor supply system; (B) a cross-sectional view of the observation chamber. In B, the upper left inset shows a closeup view of the cleaved AgI crystal attached to the upper Cu plate using heat grease; the upper center inset shows a photomicrograph of Ih ice crystals grown heteroepitaxially on the AgI crystal; the upper right inset shows the morphology of the Ih ice crystal. The surface of the cleaved AgI crystal was observed from below through a glass window that was tilted to prevent the appearance of interference fringes. Sample ice crystals on the cleaved AgI crystal were ≥16 mm distant from the source ice crystals prepared on the lower Cu plate.

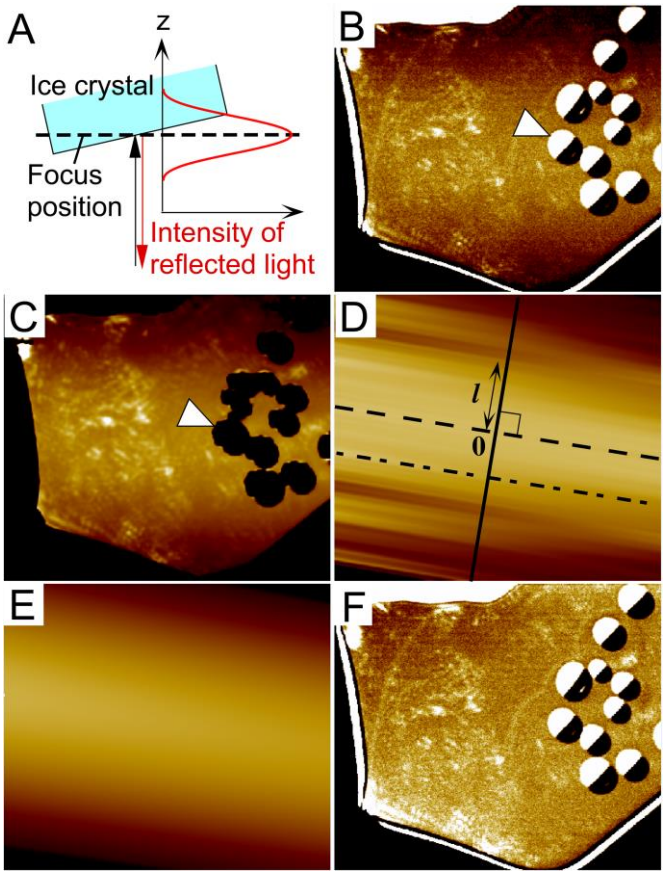

Fig. S2. Image processing performed to obtain LCM-DIM images presented in this paper (this figure was reprinted from Fig. S3 of ref. (12)). It is practically impossible to locate an ice crystal whose surface is perfectly perpendicular to the optical axis. This slight misalignment provides an inhomogeneous intensity of reflected light, as shown in A and B. In particular, in the case of confocal microscopy, the inhomogeneity of reflected light becomes significant because of its small focal depth. The area just at the focus position of an objective shows the highest intensity of reflected light. But with increasing distance from the just focused position, the intensity of reflected light significantly decreases, as A and B demonstrate. Hence, to visualize an ice crystal surface homogeneously, we corrected the inhomogeneous intensity distribution of reflected light. We obtained LCM-DIM images as a movie composed of a series of still images (4,096 gray levels) taken over a certain scan time. Then using commercial software (SPIP, Image Metrology A/S) and plug-in software (PlugIn_SnowCorr, specially written by M. Yokomine of TOYO Corporation), we carried out the image processing as follows.

1) From the original image (B), first we eliminated the pixels whose spatial gradients of reflected light intensity were steeper than 200 gray levels/pixel as spike noise, and also removed the pixels whose reflected light intensities were higher than 4,000 gray levels, which corresponded to the areas

whose gray levels were saturated (like the upper-left halves of droplets marked by white arrowheads in B and C). Then we calculated a time-averaged image (C).

2) Next, we calculated the line along which pixels had maximum intensity (dashed line shown in D). Then, along lines that were parallel to the maximum-intensity line (such as the dashed-dotted line in D), the reflected light intensities were fitted with a linear function. During the linear fitting, only the pixels, whose gray levels were present in the range of twice the standard deviation of the intensity distribution, were calculated: i.e. the portions outside a crystal surface and inside α-QLLs were eliminated from the calculation. The image D was obtained by laying (arranging) reflected light intensities approximated by the line fittings side-by-side.

3) According to the imaging theory of confocal microscopy (22), the relation between the reflected light intensity distribution I and depth z (along the optical axis) can be expressed as (shown schematically in A)

$$I(z) = \left| \frac{\sin(kz)}{kz} \right|^2. \qquad (1)$$

Here k is a constant determined by the wavelength, refractive indices, and the numerical aperture of the objective. Hence, in D, the intensity distribution along the solid line that was perpendicular to the maximum dashed intensity was fitted with the following equation

$$\frac{I(l)}{I_{l=0}} = \left| \frac{\sin(a \cdot l)}{a \cdot l} \right|^2. \qquad (2)$$

Here, l is a distance along the solid line in D ($l = 0$ at the position of the dashed line), $I_{l=0}$ is the intensity at $l = 0$, $I(l)$ is the intensity at l, and a is a fitting parameter. Then we obtained the image shown in E, in which the discontinuities in intensities shown in D were smoothed.

4) Finally, we subtracted the image E from the original image B, and adjusted the gain and offset of the subtracted image to obtain the final image shown in F.

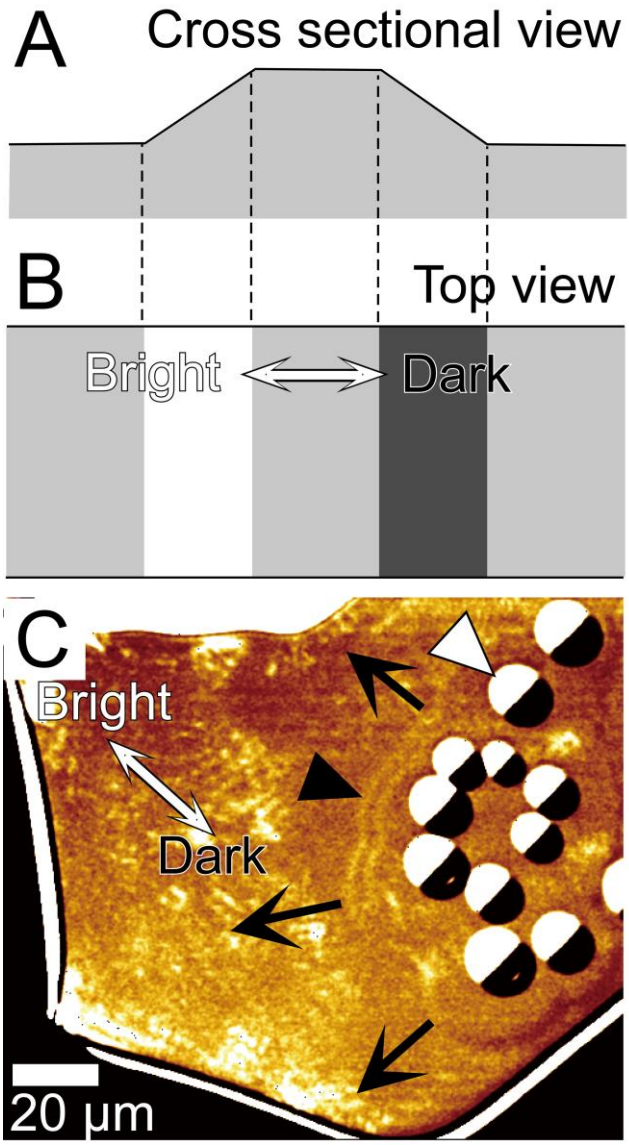

Fig. S3. Differential interference contrast (this figure was reprinted from Fig. S5 of ref. (12)). Utilizing interference of polarized light, differential interference contrast microscopy provides the contrast level so that slopes of one side and another side of a convex object look brighter and darker (white arrow), respectively, as schematically shown in A and B (as if a sample surface is illuminated from one slanted direction). Hence, in all LCM-DIM images shown in this study, the upper-left sides of the drops and steps look brighter and the lower-right sides of them look darker (a white arrow), as shown in C. In C, other arrows and arrowheads are the same as those in Fig. 1.

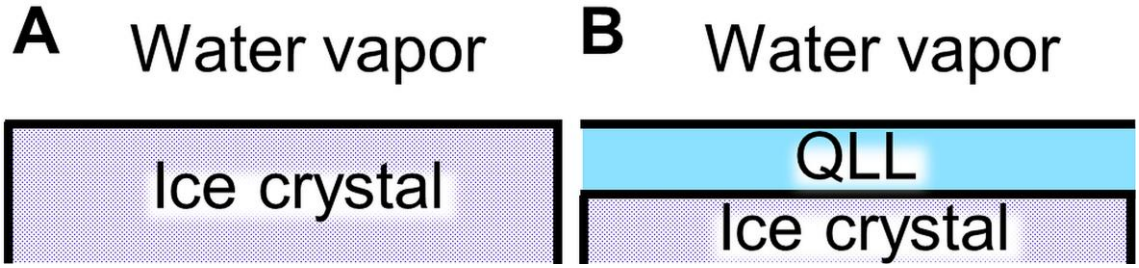

Fig. S4. The conventional picture of surface melting. Lacmann and Stranski first gave a thermodynamic explanation for the wetting of ice crystal surfaces with QLLs (19). Then Kuroda and Lacmann developed this idea into an explanation of the morphologies of snowflakes (2, 21). Kuroda and Lacmann assumed that one QLL phase fully covers an ice surface at the solid-vapor equilibrium P_{H2O}. The thickness of QLLs is at most in the order of several tens of nanometers (23). Hence, free energies of interfaces play a crucial role, in addition to those of bulk phases.

As a rough approximation, Kuroda and Lacmann presumed bulk free energy of QLLs to be that of liquid water. It is still unclear whether their approximation is appropriate. However, it seems reasonable to assume that the bulk free energy of QLLs is higher (less stable) than that of ice crystals.

When there is no QLL (A), there exists one interface between ice and vapor. In contrast, when an ice surface is covered with a QLL (B), there exist two interfaces: a QLL-ice interface and a QLL-vapor interface. The free energy of a QLL-ice interface is smaller (more stable) than that of an ice-vapor interface, since the structures of a QLL and an ice are more similar than those of an ice and vapor. In addition, the free energy of a QLL-vapor interface is also smaller (more stable) than that of an ice-vapor interface for the same reason. Therefore, Kuroda and Lacmann assumed that there should exist the case in which the sum of the free energies of QLL-ice and QLL-vapor interfaces is smaller (more stable) than the free energy of an ice-vapor interface: an ice crystal surface is fully wetted with a QLL (complete wetting). Kuroda and Lacmann evaluated the wettability of a QLL on ice crystal surfaces utilizing values of interfacial free energies determined previously (23), which lead to the expectation that the assumption of complete wetting was valid.

Taking into account the contributions of both a bulk (unstable) and interfaces (stable) of a QLL, Kuroda and Lacmann assumed that a QLL and an ice can be in equilibrium at the solid-vapor equilibrium P_{H2O}: a QLL can stably exist on an ice surface at equilibrium P_{H2O}. In addition, taking into account the effects of kinetics, Kuroda and Lacmann also presumed that a QLL can exist under both undersaturated and supersaturated P_{H2O} conditions.

The reason why Kuroda and Lacmann felt justified in the assumption of complete wetting was mainly due to the overestimation of free energy of an ice-vapor interface. With respect to this issue, see the main text.

Table S1. Previous studies on the formation of QLLs on ice crystals: all these studies showed a significant increase in the thickness of QLLs with increasing temperature, although such increase showed considerable variation depending on the measurement methods and researchers; there also exist many studies on QLLs by molecular dynamics and theoretical calculations, although such studies are not listed here; in experimental condition, S, E and U show supersaturated, equilibrium and undersaturated conditions for ice crystals, respectively

Measurement method	Reference	First author (experimental condition)
Proton channeling	(24, 25)	G (S)
Proton backscattering	(26, 27)	F (U)
Ellipsometry	(23, 28)	F (U), B (E)
X-ray diffraction	(29)	K (E)
Glancing-angle X-ray scattering	(30, 31)	D (U)
Quasi-elastic neutron scattering	(32)	M (E)
Photoelectron spectroscopy	(33, 34)	N (E), B (E)
Nuclear magnetic resonance	(35, 36)	K (E), M (U)
Optical microscopy	(37, 38)	E (S), G (S)
Optical displacement sensor	(39)	K (U)
Infrared spectroscopy	(40)	S (S)
Sum-frequency vibrational spectroscopy	(41, 42)	W (E)
Atomic force microscopy	(43-46)	B (S), D (U), S (U, E, S), P (E)

Video S1. The appearance of round liquid-like droplets (*a*-QLLs) and thin liquid-like layers (β-QLLs) on an ice basal face under relatively high supersaturation conditions (P_{H2O}=585 Pa, σ=13 %) at T_{sample}=-2.0 °C. Basal faces were observed by LCM-DIM. Photomicrographs of 660×508 pixels were acquired over a 2.2-s time interval.

Video S2. The disappearance of a thin liquid-like layer (β-QLL) on an ice basal face under relatively medium supersaturation conditions (P_{H2O}=568 Pa, σ=10 %) at T_{sample}=-2.0 °C. After Fig. 1 was taken, P_{H2O} was reduced from 585 to 568 Pa, keeping T_{sample} constant. Then, basal faces were observed by LCM-DIM. Photomicrographs of 624×258 pixels were acquired over a 9.8-s time interval.

Video S3. The disappearance of a round liquid-like droplet (α-QLL) on an ice basal face under relatively low supersaturation conditions (P_{H2O}=532 Pa, σ=3 %) at T_{sample}=-2.0 °C. After Fig. 2 was taken, P_{H2O} was reduced from 568 to 532 Pa, keeping T_{sample} constant. Then, basal faces were obsereved by LCM-DIM. Photomicrographs of 504×492 pixels were acquired. To demonstrate the disappearance of the α-QLL efficiently, a time interval between adjacent frames is not regular.